Gregory S. Rohrer and Chang-Soo Kim

Department of Materials Science and Engineering, Carnegie Mellon University, Pittsburgh, Pennsylvania, USA

The Influence of Singular Surfaces and Morphological Changes on Coarsening

When the interface energy between coarsening crystals and an intervening phase is anisotropic, mechanisms that do not affect isotropic systems become important. If there are singular surfaces, then growth and dissolution must occur by the lateral motion of steps, formed at a defect center or by two-dimensional nucleation. Here, it is shown that two-dimensional nucleation is not plausible under typical experimental conditions and that persistent step creating defects are required for a singular surface to advance or retract during coarsening. The simultaneous presence of crystals with and without defects leads to two populations that grow at very different rates and this provides an explanation for abnormal coarsening. The influence of extrinsic morphological changes is also considered. It is assumed that when relatively high energy, non-equilibrium shapes in the starting materials evolve during coarsening to shapes increasingly bound by lower energy surfaces, the mean surface energy is reduced. Simulations show that under these conditions, non-classical coarsening kinetics arise in which the rate constant decreases linearly with the mean surface energy.

Keywords: Coarsening; Surface energy; Nucleation; Morphology

Version 10/20/04: accepted for publication in a special issue of „Zeitschrift für Metallkunde“ dedicated to Prof. Dr. Duk Yong Yoon on the occasion of his 65th birthday.

1. Introduction

One of Professor Dr. Duk Yong Yoon's important contributions to our field has been the experimental demonstration that interface structure in general, and the roughening transition in particular, influence microstructural evolution during grain growth and coarsening [1-11]. Furthermore, he has also identified a robust link connecting singular surfaces to abnormal coarsening and grain growth phenomena. Based on this work, abnormal growth can be attributed to the step migration growth mechanisms of singular surfaces [11]. The variations in interface structure studied by Yoon are quite general and will occur in any system where the interface energy as a function of the surface normal, $\gamma(\mathbf{n})$, contains one or more singularities. In this paper, we intend to honor Prof. Yoon by describing the results of coarsening simulations that examine the effects of nucleation limited growth and of morphological variations that are a direct consequences of interface energy anisotropy.

In the classical coarsening theory, the average crystal size $\langle r \rangle$ increases with time:

$$\langle r \rangle^n - \langle r_0 \rangle^n = Kt, \qquad (1)$$

where K is the positive growth rate constant, $\langle r_0 \rangle$ is the initial average radius, and n is a constant greater than or equal to two that depends on the rate limiting step of the process [12,13]. In either case, a statistically self similar distribution results where the maximum crystal size is 1.5 times the average size (for diffusion limited coarsening) or 1.8 times the average size (for surface attachment limited coarsening). Although the original derivation of this law assumes isotropic interface energies, Mullins [14] has shown that as

long as the crystal size distributions maintains statistical self-similarity and the interface energy is differentiable at all orientations, then the anisotropy of the interface energy does not alter the kinetics described by Eq. 1. Furthermore, a one dimensional capillary-driven growth model demonstrated that for anisotropic boundary properties, a statistically self similar particle size distribution is obtained and that the distribution is different from that which results from uniform boundary properties [15]. Two-dimensional coarsening models have also indicated that the crystal size distribution is influenced by interface energy anisotropy [16,17]. These results reproduced Mullins' predictions that anisotropy does not affect growth kinetics, but does weakly influence the distribution of crystal sizes.

These results, referred to here as the classical theory of coarsening, stand in stark contrast to what is actually observed in many ceramic systems. For example, bimodal grain size distributions are frequently reported in which some abnormal grains are more than 100 times the size of the average of the majority population. Furthermore, the growth constant (K in Eq. 1) for the abnormal grains has been reported to be as much as 100 times that of the majority grains in the same material [18]. This phenomenon has been used to grow single crystals of ceramics by annealing a seed crystal in contact with a polycrystalline material and a lower melting intergranular liquid; the most well documented case is that of $Pb(Mg_{1/3}Nb_{2/3})O_3 - x\ PbTiO_3$ (PMN/PT) [19-21]. Kinetic data suggests that there is a continuous reduction in the growth rate beyond that predicted by Eq. 1, as if the growth constant, K, is decreasing by a factor of five from the initial to the final stages of the process [22]. It has also been shown that the evolution of porosity does not entirely explain the reduction in the growth rate [23].

In this paper, we propose that both the bimodal distribution and the decreasing growth rates can be explained by the presence of singular surfaces and non-equilibrium morphologies. These effects are not captured by the theories cited above because of the assumptions on which the theories were developed. First, if the surface energy is not differentiable at all points, then there will be flat, singular surfaces that can only advance or retreat by the lateral motion of steps. In the absence of defects, these steps must be created by nucleation. If nucleation is slow or energetically not feasible, then those crystals with persistent step sources (screw dislocations or twin plane reentrant edges) are expected to grow at a much faster rate than those without and this can lead to a bimodal grain size distribution. Second, if the distribution of grain shapes evolves to morphologies bounded by slower moving, lower energy interfaces, then we can expect the driving force for growth to decrease and this is expected to lead to a continuous reduction in the growth constant. Recent observations support this idea. Measurements of the distribution of $SrTiO_3$ surfaces, when coarsening in a TiO_2-rich eutectic liquid, and the distribution of PMN/PT surfaces, when coarsening in a PbO rich liquid, showed that approximately isotropic initial shapes continuously evolve to more polygonal forms bounded by low energy surfaces [22,24]. In the next section, the results of earlier calculations [25] illustrating the effect that singular surfaces have on coarsening are reviewed and, in section 3, new results are presented that illustrate how the evolution of grain shapes affects coarsening.

2. Nucleation limited coarsening theory

The theory for nucleation limited coarsening was originally described elsewhere [25]. In the current paper, we review the underpinnings of the theory by deriving simplified expressions for the barriers for growth and dissolution during coarsening and then compare the predictions from numerical models to the results of some recent experiments. We begin with a consideration of how nucleation on a singular interface affects the coarsening of crystals bounded by singular interfaces. To simplify the situation, we assume that we begin with a collection of cube shaped crystals with surface energy γ and a distribution of edge lengths, L. The crystals are dispersed in an intervening phase and the chemical potential of the material dissolved in that phase is $\mu_\infty = 2\gamma r^*$. The system is assumed to be sufficiently dilute so that all crystals are surrounded by the same mean field chemical potential, μ_∞. Therefore, there is a crystal size, $L^* = 2r^*$, that is in equilibrium with the intervening phase. We can now consider the energy involved in transferring material from the intervening phase to the surface of a crystal. To do this, we place a square nucleus of area s^2 and height a on the flat facet, where the chemical potential is zero. The energy for this transfer is:

$$\Delta G(s) = 4as\gamma - as^2 \frac{2\gamma}{r^*}, \qquad (2)$$

for $0 \le s \le L$. In Eq. 2, the first term on the right hand side is the energy of the perimeter of the nucleus and the second term is the change in the free energy on moving a volume of material (as^2) from the intervening phase to the flat surface. Equation 2 shows that the energy change on adding a complete layer ($s = L$) to a crystal with size $L = 2r^*$ is zero, as

expected; however, before the layer is completed, the crystal must past through a relatively higher energy state that contains a partial layer. By differentiation, we see that the maximum occurs at $s = r^*$ and that the barrier to addition is $\Delta\gamma_+ = 2a\gamma r^*$, where $0 < r^* < L$. It is important to note that the barrier for adding layers is independent of the size of the growing crystal and governed entirely by r*, which is a measure of the average size of the crystals in the system.

To remove material from the crystal and dissolve it in the intervening phase, the change in energy is:

$$\Delta\gamma(s) = 4as\gamma - 4aL\gamma + (aL^2 - as^2)\frac{2\gamma}{r^*} \tag{3}$$

In Eq. 3, the first two terms on the right hand side represent the energy difference between a complete layer and a partial layer; this energy is ≤ 0 for all valid values of s. The final term on the right hand side is the energy increase associated with moving a volume of material from the flat surface to the reservoir. It can be shown that the maximum of Eq. 3 is at $s = r^*$ and the barrier to removing a layer, $\Delta\gamma_-$, is:

$$\Delta\gamma_- = 2a\gamma\left(r^* + L\left(\frac{L}{r^*} - 2\right)\right) \tag{4}$$

where $r^* \leq L \leq 2r^*$. Note that for a crystal of size $L = 2r^*$, $\Delta\gamma_+ = \Delta\gamma_- = 2a\gamma r^*$, as expected for the equilibrium case. For smaller crystals, the barrier decreases (see Fig. 1) and vanishes completely for crystals with $L = r^*$. A more generalized form of these barriers has been

derived previously, but the simplified forms given above are acceptable for the present purposes and do not lead to different conclusions [25].

It is first important to compare the size of these barriers to the available thermal energy and the potential energy supplied by capillarity. The most important barrier is the one for the growth of crystals with sizes ≥ $2r^*$ (this is the largest barrier). Even though small crystals can shrink without a barrier, the constraint of mass conservation will restrict their ability to do so if the barrier for growth is too large. In a typical situation that might be realized in the laboratory, we can take a to be 2×10^{-10} m, γ to be 1 J/m^2, and r^* to be 500 nm. To a first approximation, the choice of r^* is set to the average size of the crystals in the coarsening compact and 500 nm is taken as a lower limit for most practical cases; this leads to a barrier to growth of 2×10^{-16} J. The relevant energies for comparison are the energy change resulting from capillarity driven growth (taken to be $2\gamma a^3/r^* = 3 \times 10^{-23}$ J) and the available thermal energy ($kT = 2 \times 10^{-20}$ J at 1500 °C). Although these calculations are admittedly approximate, several things are clear. First, since the barrier energy for growth on micron sized crystals is more than 10^6 times the capillary driving force, we can be certain that capillarity cannot drive nucleation. In fact, for all cases where the grain size is larger than a few nm, if nucleation occurs, it must be driven by thermal fluctuations. The second point is that even thermal fluctuations are unlikely to drive nucleation on large crystals. According to the estimates above, the nucleation energy barrier is $10^4 kT$. It has been estimated that barriers greater than $40kT$ are not overcome in reasonable time periods [26]. It should be noted that the step edge energy is usually thought to be a fraction of the surface energy, so the barrier height is probably over estimated. However, the nucleus perimeter energy would have to be

reduced by a factor of 100, to 0.01 J/m^2 before the barrier would be reduced to 40kT. Since this is considered unlikely, the size of the barrier energy and the extremely small driving force implies that singular interfaces without defects should never advance outward during coarsening [27].

For comparison, we should also consider the conditions under which two dimensional nucleation can be expected to occur and has been observed experimentally. The theory for two-dimensional nucleation shows that the nucleation rate decreases exponentially as the ratio of the driving force to the available thermal energy decreases and as the ratio of the perimeter energy to the available thermal energy increases [28]. In accordance with the theory, two-dimensional nucleation has been observed in cases where driving forces comparable to the thermal energy are provided by supersaturated liquids or vapors, or by cooling a melt below the crystallization temperature. For example, growth by two-dimensional nucleation has been reported during the solidification of liquid Ga, where the driving force is supplied by the latent heat of crystallization, which is greater than the available thermal energy [29,30]. In this case, it is also relevant to note that solid-liquid interface energy is very low (in the range of 0.04 to 0.07 J/m^2) and that the nucleus perimeter energy was determined to be in the range of 0.01 to 0.02 J/m^2. So, in addition to a high driving force, the nucleation energy barrier is significantly reduced by the low interfacial energy. Two-dimensional nuclei have also been observed on barium nitrate surfaces by atomic force microscopy, and in this case it was inferred that the nuclei formed during a period of very high supersaturation that occurred when the crystal was removed from the growth solution [31]. During this uncontrolled period of growth, it is difficult to estimate the driving force for

crystallization. The transition from dislocation controlled growth to two-dimensional nucleation controlled growth has been observed during the vapor deposition of NaCl, where it is possible to estimate that driving force [32]. It was reported that the transition to two-dimensional nucleation occurs when the driving force exceeds 0.09 eV at 347 °C. At this point, the driving force is approximately twice the thermal energy. In summary, two-dimensional nucleation has been observed in the past when the driving force is relatively large and comparable to the available thermal energy. In contrast, the capillary driving forces that arise during the coarsening of micron-sized crystals are only a small fraction of the thermal energy.

Several authors have argued that the growth mechanisms associated with singular interfaces can be used to explain abnormal growth phenomena. Through the analysis of microstrutural data from many different systems, Yoon and co-workers [11] have noted that abnormal growth phenomena occur when singular interfaces are present in the system and that systems with fully rough interfaces grow normally. Their explanation is that abnormal growth is attributed to the step migration growth mechanisms of singular surfaces. Two different mechanisms have been invoked. The first, articulated in Ref. 33 and citations therein, is that some grains can become large enough that the capillary driving force is higher than the critical value for the onset of nucleation, and this leads to abnormal growth. However, based on the numerical estimates made in the paragraph above, this explanation is not viable. One reason is that under typical experimental conditions, the energies associated with thermal fluctuations are much larger than the capillarity driving force so that nucleation will be driven by thermal fluctuations or not at all. Another reason that the explanation is not viable is that all growing crystals are

subject to the same barrier ($\Delta_+ = 2a\gamma^*$) so that the size of the growing crystal is simply not a relevant factor; if two-dimensional nucleation is energetically possible on one growing crystal then it will occur on all growing crystals exposed to the same mean field chemical potential. The second possible mechanism is that step producing structural defects, expected to occur in a subset of the crystals, allow the defective population to grow without a barrier and the average size of this subset becomes much larger than the more perfect crystals. It seems clear that having two distinct populations growing at very different rates is a plausible explanation for abnormal growth. However, a subset of large crystals growing by capillarity driven two-dimensional nucleation is not plausible.

The defect controlled coarsening mechanism has been studied in detail and numerical simulations based on this model have demonstrated its feasibility [25]. In the case where the growth of mixed populations are modeled (some crystals are limited by the barrier and others are assumed to have defects) bimodal populations are observed where the defect containing subset of crystals grows much faster than the others, as illustrated in Fig .2. Note that because the smallest crystals in the slow population are able to shrink without a barrier (see Eq. 4) they sustain the growth of the minority population of defective crystals.

The nucleation limited coarsening model makes a number of predictions that can be compared to experiment. The first is that abnormal growth should be transient. In other words, at some point the defective (fast growing) grains have completely consumed the ideal (slow growing) population; because none of the remaining population has an advantage, growth should then proceed normally. The second is that during the period of bimodal growth, the number density of the large grains should remain constant while the

number of small grains should decrease. Although detailed measurements of the evolution of the grain size distribution are not yet available, some reports in the literature are consistent with this model [18].

The dislocation density in large $SrTiO_3$ seed crystals has been correlated with the rate at which they grow into a polycrystalline compact [34]. Although there were only two observations, the seed with a higher dislocation density had a higher growth rate. Orientation imaging microscopy data suggest that all abnormal grains in PMN/PT have a twin (a boundary with a 60° rotation about <111>). Twins are not found in the smaller matrix grains [21, 35] and these observations have been used to suggest that the reentrant twin plane edge provides a nucleation site with a greatly reduced barrier that allows the twinned crystals to grow much faster than the untwined crystals. However, it should be noted that by only observing the final state, it is not possible to determine if the twin caused the grain to become large or if twins arise naturally in all grains when they become large. It can be reasoned that any grain that grows large enough will have encountered grains of many other orientations. In a random orientation distribution, approximately 1 in 50 misorientations will be close to the twin relationship [36]. Thus, if a grain grows so that it has encounters many more than 50 differently oriented grains, it is likely that a twin will be formed and this may be the reason that all large grains have twins. The independence of twinning and high growth rates was demonstrated in a recent paper where it was shown that there is no measurable difference in the growth rates of twinned and untwined seeds [37]. Since these seeds were relatively large, it is likely that they contained screw dislocations that could act as persistent step sources.

While the habit plane of the twin in PMN/PT is incoherent, $BaTiO_3$ forms very straight coherent twins on {111} planes. When $BaTiO_3$ compacts are seeded with twined grains, the twined seed outgrew the untwined seeds, suggesting that a reentrant twin plane edge nucleation mechanism promotes abnormal growth [38]. This is also suggested by observations of $BaTiO_3$ coarsened at temperatures in the range of 1350 °C (where an intergranular liquid is expected to form), which showed that twinned grains grow larger than others [39]. Rehrig et al. [18] independently measured the grain sizes of the large and small populations and showed that within experimental error, the sizes of the small grains had stopped growing while the large grains continued to increase in size. It should be noted that while the ideal version of the nucleation limited coarsening theory suggests that the growth of ideal (smaller) crystals should completely cease when they reach a size where the nucleation energy barrier becomes insurmountable (and this size should be in the nanometer size range), it does not account for finite volume fraction effects and growth from coalescence that is expected even in the absence of nucleation. In other words, there may be some growth by grain boundary migration, even in the absence of coarsening. For a rigorous comparison to the theory, it remains necessary to evaluate the complete crystal size distribution and volume density as a function of time. This work is currently being carried out in our laboratory.

3. Effect of Morphological Variations

In this section, we first examine how a distribution of crystal morphologies influences coarsening and then how a continuous change in the average morphology influences coarsening. The algorithm and physical parameters used for the numerical

simulations presented in this paper are described in detail in a previous publication [25]. All of the results presented in this section were computed under the assumption that all of the growing crystals have step producing defects that allow growth. In other words, there is no nucleation energy barrier to restrict growth. This situation is expected to apply either to the growth of a large seed (guaranteed to have screw dislocations by virtue of its size) in a matrix of finer source material or to a collection of grains with persistent step sources that survives after an initial transient of bimodal growth. When this algorithm is used to simulate coarsening with a constant surface energy for all of the crystals, it produces an average grain size that increases as $t^{1/3}$ and the time invariant crystal size distribution predicted by the classical theory [12,13].

First, we consider morphological distributions that are likely to occur during the coarsening of non-isotropic crystals. It is reasonable to expect that because of differences in the atomic mechanisms of growth and dissolution, not all crystals in a coarsening system will have the same shape. For example, we expect the shapes of the growing crystals to be dominated by the slowest growing facet. These same facets will shrink and disappear from the dissolving crystals. Since the slow growing facets are most frequently the low energy facets, it is reasonable to expect that the average surface energy of the growing crystals will be lower than that of the dissolving crystals and this will influence the driving force for exchange of material with the intervening phase. This was simulated by assigning different average surface energies to different size classes according to the following function:

$$\gamma(r) = \gamma_0 \left(\frac{1/2}{1 + exp\left[(r - r^*)/\Delta \right]} + \frac{1}{2} \right) \qquad (5)$$

Where γ_0 is the mean surface energy of the smaller crystals, the mean energy of the larger crystals is one half this value, and δ is a measure of the width of the transition region between the higher and lower energy and is measured in the same units as r. The mean surface energy (γ) as a function of reduced radius is plotted in Fig. 3a for δ = 2 (a narrow transition) and δ = 5 (a broader transition).

The kinetic results are summarized in Fig. 4, where it is clear that the growth in all of these systems follows classical, diffusion controlled ($t^{1/3}$) kinetics. These results are consistent with Mullins' [14] prediction that a distribution of crystal shapes does not affect the growth exponent. According to the data in Fig. 4, the systems with distributed surface energies grew more slowly than the system with a constant surface energy. This is not because the energies are distributed, but because the mean values of the energies of these systems are 25 % lower than that of the system with a constant energy.

The crystal size distributions are plotted in Fig. 3b. Each of these distributions represents that same volume of material. The distribution for the system with the constant energy (the solid line) matches the classical result [12, 13]. The distributions for the systems with distributed surface energies are both narrower. However, the changes are rather subtle and would be difficult to observe in a measured crystal size distribution. Therefore, if a system of coarsening crystals possesses a range of crystal sizes and shapes, the observable crystal size distribution is not significantly affected and the kinetics are not changed at all; the existence of a range of crystal shapes can therefore be ruled out as an explanation for non-classical coarsening.

Next, we considered the influence of continuous changes in morphology. Although this is an extrinsic phenomenon that results from sample history, it is probably unavoidable in most practical situations and it is therefore useful to understand the ramifications. When materials are prepared for a coarsening experiment, it is standard practice to grind or mill the starting powders. As result, the initial shapes are expected to be more or less equiaxed. As growth occurs, the particles will be increasingly bounded by slow growing facets. Indeed, the extent of these processes have been reported in two recent studies [22, 24]. Based on these observations, we assume that the crystals will evolve to more energy minimizing shapes, thus resulting in a steady decrease in the mean surface energy per area. Therefore, we consider here the coarsening of crystals that all have the same energy at any point in time, but whose mean surface energy per area is decreasing linearly with the reduced grain size, $\square = r/r^*$. Two cases are considered. In the first, it is assumed that the mean surface energy decreases by 10 % while the reduced grain size increases by a factor of 10. In the second, it is assumed that the surface energy decreases by 50 % in the same size interval.

The crystal size distributions resulting from these simulations, when normalized by volume, all reproduced the classical results and are not shown [12, 13]. Therefore, we can conclude that morphological changes will not affect the distribution of crystal sizes. On the other hand, the kinetics are affected. The cube of the average grain size is plotted as a function of time in Fig. 5a. The slopes of these lines give the growth constants (K in Eq. 1) for each system. After an initial transient, the system with the constant energy (black line) has a constant slope, indicating that K is constant, as expected for classical kinetics. The systems with the changing surface energy have a continuously decreasing

growth constant. The growth constant was calculated at each point in time by the finite difference method and the results are depicted in Fig. 5b. From this result, we see that the growth constant decreases by the same amount as the surface energy over the same time interval. This is because the capillary driving force is reduced in proportion to the surface energy. It should be noted that in a real system, the decrease in the mean surface area is not expected to be linear with the average grain size. Instead, we expect a rapid decrease in the initial stages of heating, followed by more subtle changes later in the process. However, this does not alter the conclusion that the overall decrease in the driving force reduces K. This phenomenon provides a plausible explanation for the unexplained reduction in growth rate observed in the PMN/PT system [22].

4. Summary and Conclusions

The energy requirements for two-dimensional nucleation on a singular surface are compared to the potential energy supplied by capillarity and available thermal energy under typical experimental conditions. Based on this comparison, it is not plausible for capillary driving forces to drive two dimensional nucleation during coarsening. The simultaneous presence of crystals with and without defects leads to two populations that grow at very different rates and this provides an explanation for abnormal coarsening. Simulations show that extrinsic changes in the average surface energy lead to non-classical coarsening kinetics and a decreasing coarsening rate constant. The decrease in the rate constant scales linearly with the decrease in the surface energy and the crystal size distribution is unchanged.

This work was supported primarily by the MRSEC program of the National Science Foundation under Award Number DMR-0079996 and partially by NASA under grant number 8-1674.

References

[1] Y.K. Cho, S.-K.L. Kang, D.Y. Yoon: J. Am. Ceram. Soc. 87 (2004) 119.

[2] Y.K. Cho, D.Y. Yoon: J. Am. Ceram. Soc. 87 (2004) 438.

[3] Y.K. Cho D.Y. Yoon: J. Am. Ceram. Soc. 87 (2004) 443.

[4] M.J. Kim, Y.K. Cho, D.Y. Yoon: J. Am. Ceram. Soc. 87 (2004) 455.

[5] M.J. Kim, Y.K. Cho, D.Y. Yoon: J. Am. Ceram. Soc. 87 (2004) 507.

[6] C.W. Park, D.Y. Yoon, J.E. Blendell, C.A. Handwerker: J. Am. Ceram. Soc. 86 (2004) 603.

[7] M.J. Kim, D.Y. Yoon: J. Am. Ceram. Soc. 86 (2003) 630.

[8] C.W. Park, D.Y. Yoon: J. Am. Ceram. Soc. 85 (2002) 1585.

[9] C.W. Park, D.Y. Yoon: J. Am. Ceram. Soc. 84 (2001) 456.

[10] Y.J. Park, N.M. Hwang, D.Y. Yoon: Metall. Mater. Trans. 27A (1996) 2809.

[11] D.Y. Yoon, Y.K. Cho, "Roughening Transition of Grain Boundaries in Metals and Oxides," Interface Science (2004) in press.

[12] I.M. Lifshitz, V.V Slyozov: J. Phys. Chem. Solids 19 (1961) 35.

[13] C. Wagner: Z. Elektrochem. 65 (1961) 581.

[14] W.W. Mullins: J. Appl. Phys. 59 (1986) 1341.

[15] W.W. Mullins, J. Vinals: Acta Mater. 41 (1993) 1359.

[16] A.D. Rutenberg, B.P. Vollmayr-Lee: Phys. Rev. Lett. 83 (1999) 3772.

[17] E. Brosh, R.Z. Shneck: Modelling Simul. Mater. Sci. Eng. 8 (2000) 815.

[18] P.W. Rehrig, G.L. Messing, S. Trolier-McKinistry: J. Am. Ceram. Soc. 83 (2000) 2654.

[19] A. Khan, F.A. Meschke, T. Li, A.M. Scotch, H.M. Chan, M. P. Harmer: J. Am. Ceram. Soc. 82 (1999) 2958.

[20] E.M. Sabolsky, G.L. Messing, S. Trolier-McKinstry: J. Am. Ceram. Soc. 84 (2001) 2507.

[21] J.S. Wallace, J.-M. Huh, J.E. Blendell, C.A. Handwerker: J. Am. Ceram. Soc. 85 (2002) 1581.

[22] E.P. Gorzkowski, H.M. Chan, M.P. Harmer, T. Sano, C.-S. Kim, G.S. Rohrer: "Changes in the Distribution of Interfaces in PMN- 35 mol% PT as a Function of Time," Z. Metallkd., submitted (for this issue).

[23] E.P. Gorzkowski, H.M. Chan, M.P. Harmer: "Effect of PbO on the Kinetics of {001} $Pb(Mg_{1/3}Nb_{2/3})O_3$-35mol% $PbTiO_3$ Single Crystals Grown into Fully Dense Matrices," J. Am. Ceram. Soc., submitted February 2004.

[24] T. Sano, C.-S. Kim, G.S. Rohrer: J. Am. Ceram. Soc., in press.

[25] G.S. Rohrer, C.L. Rohrer, W.W. Mullins: J. Amer. Ceram. Soc. 85 (2002) 675.

[26] W.W. Mullins, G.S. Rohrer: J. Amer. Ceram. Soc. 83 (2000) 214.

[27] B.W. Sheldon, J.Rankin: J. Amer. Ceram. Soc., 85 (2002) 683.

[28] J.D. Weeks, G.H. Gilmer, in: I. Prigogine and S.A. Rice (Eds), Advances in Chemical Physics, Vol. 40, John Wiley and Sons, New York, (1979) 157.

[29] S.D. Peteves, R. Abbaschian: Matall. Mater. Trans. 22A (1991) 1259.

[30] S.D. Peteves, R. Abbaschian: Matall. Mater. Trans. 22A (1991) 1271.

[31] K. Maiwa, M. Plomp, W.J.P. van Enckevort, P. Bennema: J. Cryst. Growth 186 (1998) 214.

[32] K.W. Keller: J. Cryst. Growth 74 (1986) 161.

[33] K.-S. Oh, J.-Y. Jun, D.-Y. Kim, N.-M. Hwang: J. Amer. Ceram. Soc. 83 (2000) 3117.

[34] S.-Y. Chung, S-J Kang: J. Amer. Ceram. Soc. 83 (2000) 2828.

[35] U.J. Chung, J.K. Park, N.-M. Hwang, H.-Y. Lee, D.-Y. Kim: J. Amer. Ceram. Soc. 85 (2000) 965.

[36] D.H. Warrington, M. Boon: Acta Met. 23 (1975) 599.

[37] D.J. Rockosi, E.P. Gorzkowski, P.T. King, A.M. Scotch, H.M. Chan, M.P. Harmer: J. Amer. Ceram. Soc. 87 (2004) 1339.

[38] M.-K. Kang, Y.-S. Yoo, D.-Y. Kim, N.-M. Hwang: J. Amer. Ceram. Soc. 83 (2000) 385.

[39] H.-Y. Lee, J.-S. Kim, D.-Y. Kim: J. Amer. Ceram. Soc. 85 (2002) 977.

Correspondence address

Gregory S. Rohrer
W.W. Mullins Professor of Materials Science and Engineering
Department of Materials Science and Engineering
Carnegie Institute of Technology
Carnegie Mellon University
5000 Forbes Ave.
Pittsburgh, Pennsylvania 15213-3890
Tel: +1 412-268-2696
Fax: +1 412-268-3113
E-mail:gr20@andrew.cmu.edu
www: www.materials.cmu.edu/rohrer

Figure Captions

Figure 1. Plot of the nucleation energy barrier for crystals of different sizes in contact with a reservoir with a chemical potential $2\gamma r^*$.

Figure 2. Simulated crystal size distribution for the defect free crystals (dashed line) and the crystals with a persistent step source (solid line) coarsening in the same system. (a) after 1 arbitrary unit of time, (b) after 8, (c) after 11. The crystals with the step source grow without a barrier.

Figure 3. (a) Plot of the mean surface energy as a function of reduced crystal size for the cases of a constant energy (solid black line), energy varying according to Eq. 5 with γ = 5 (dashed black line), energy varying according to Eq. 5 with γ = 2 (dashed gray line). (b) Resulting crystal size distributions for the cases described above.

Figure 4. Plot of the cube of the grain size as a function of time for the cases of a constant energy (solid black line), energy varying according to Eq. 5 with γ = 5 (dashed black line), energy varying according to Eq. 5 with γ = 2 (dashed gray line). These last two lines overlap.

Figure 5. (a) Plot of the cube of the grain size as a function of time for the cases of a constant energy (solid black line), energy decreasing by 50 % over the simulation interval (dashed black line), energy decreasing by 10 % over the simulation interval (dashed gray line). (b) The instantaneous growth constant for the three simulations described above.

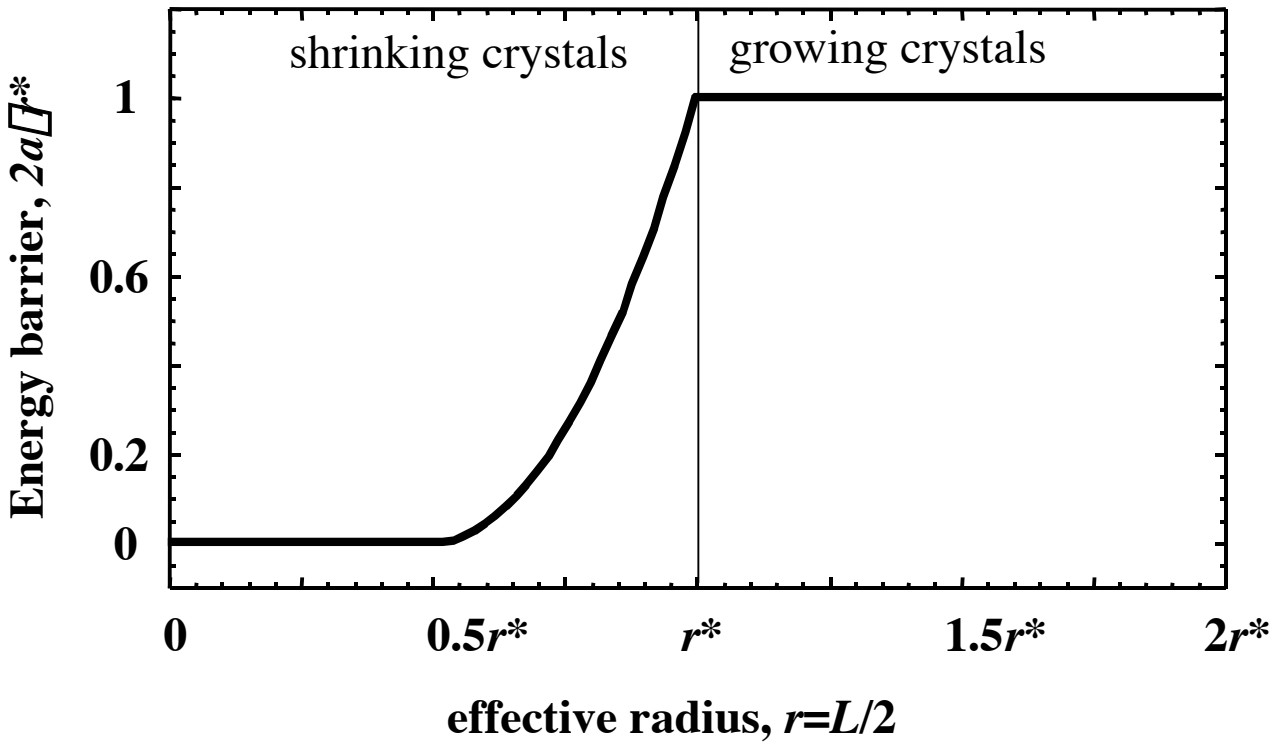
shrinking crystals
growing crystals
Energy barrier, 2a[]*
1
0.6
0.2
0
0
0.5r*
r*
1.5r*
2r*
effective radius, r=L/2

Figure 1.

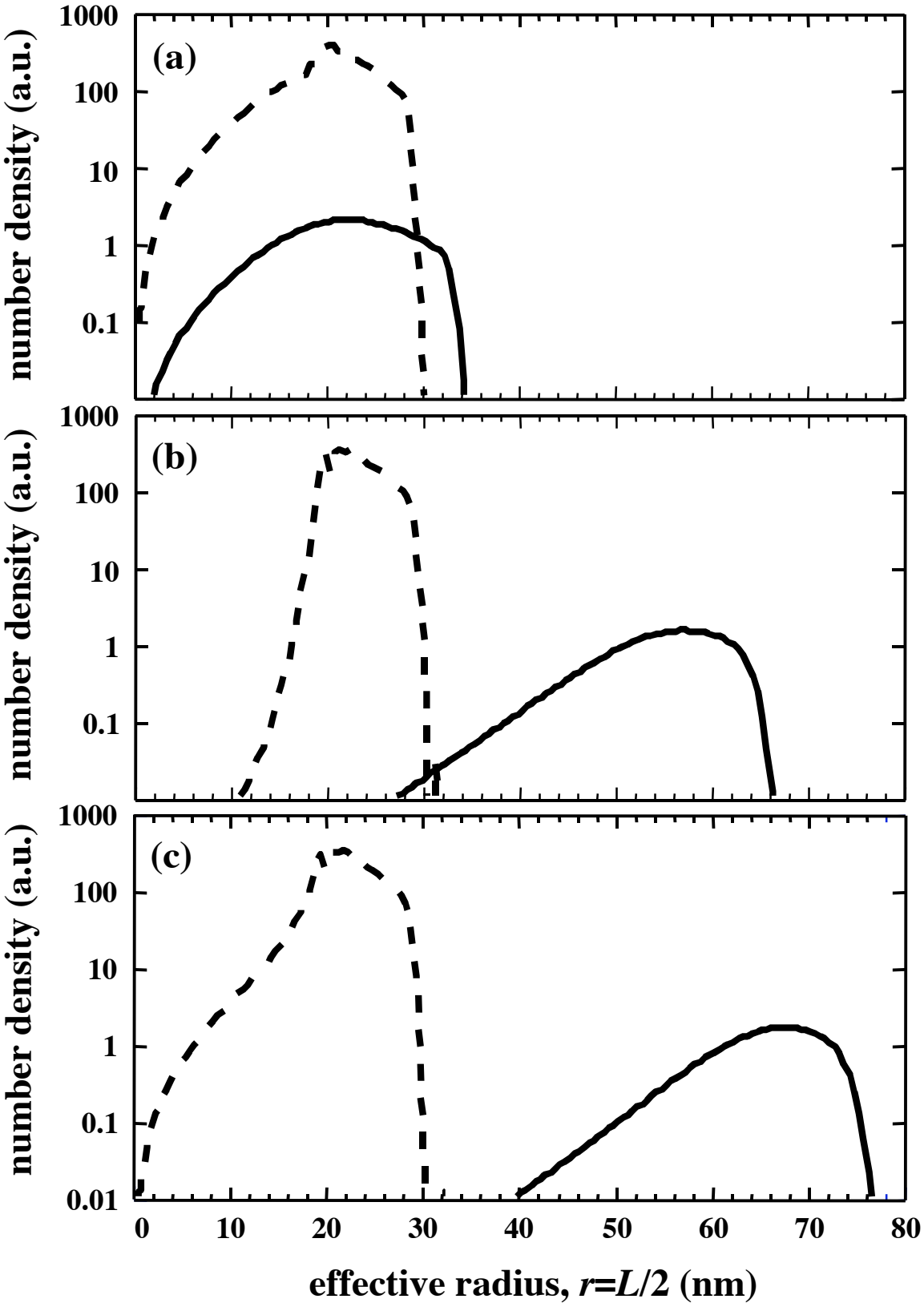
(a)
(b)
(c)
number density (a.u.)
number density (a.u.)
number density (a.u.)
1000
100
10
1
0.1
0.01
0
10
20
30
40
50
60
70
80
effective radius, r=L/2 (nm)

Figure 2.

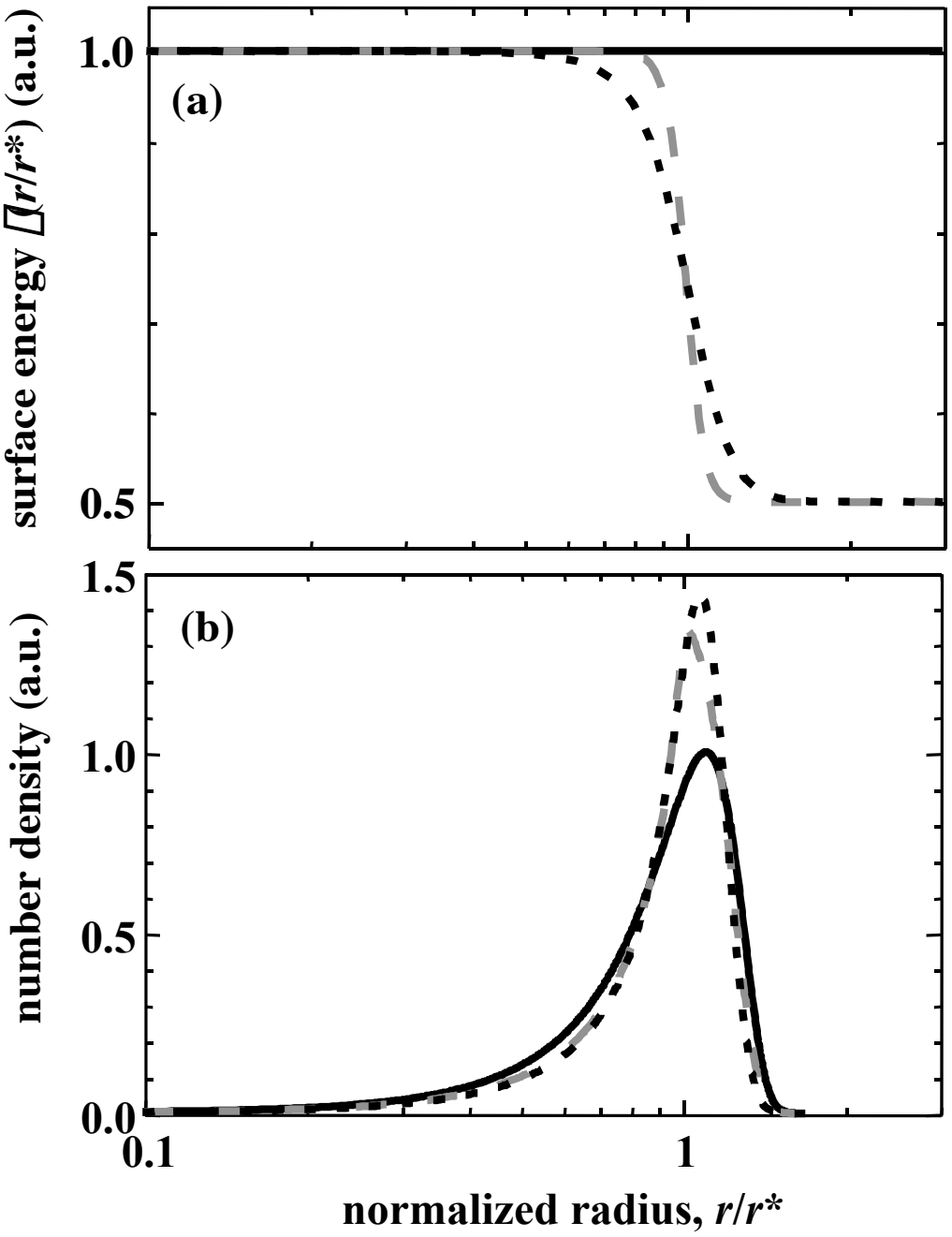
surface energy [(r/r*) (a.u.)
1.0
0.5
(a)
number density (a.u.)
1.5
1.0
0.5
0.0
(b)
0.1
1
normalized radius, r/r*

Figure 3.

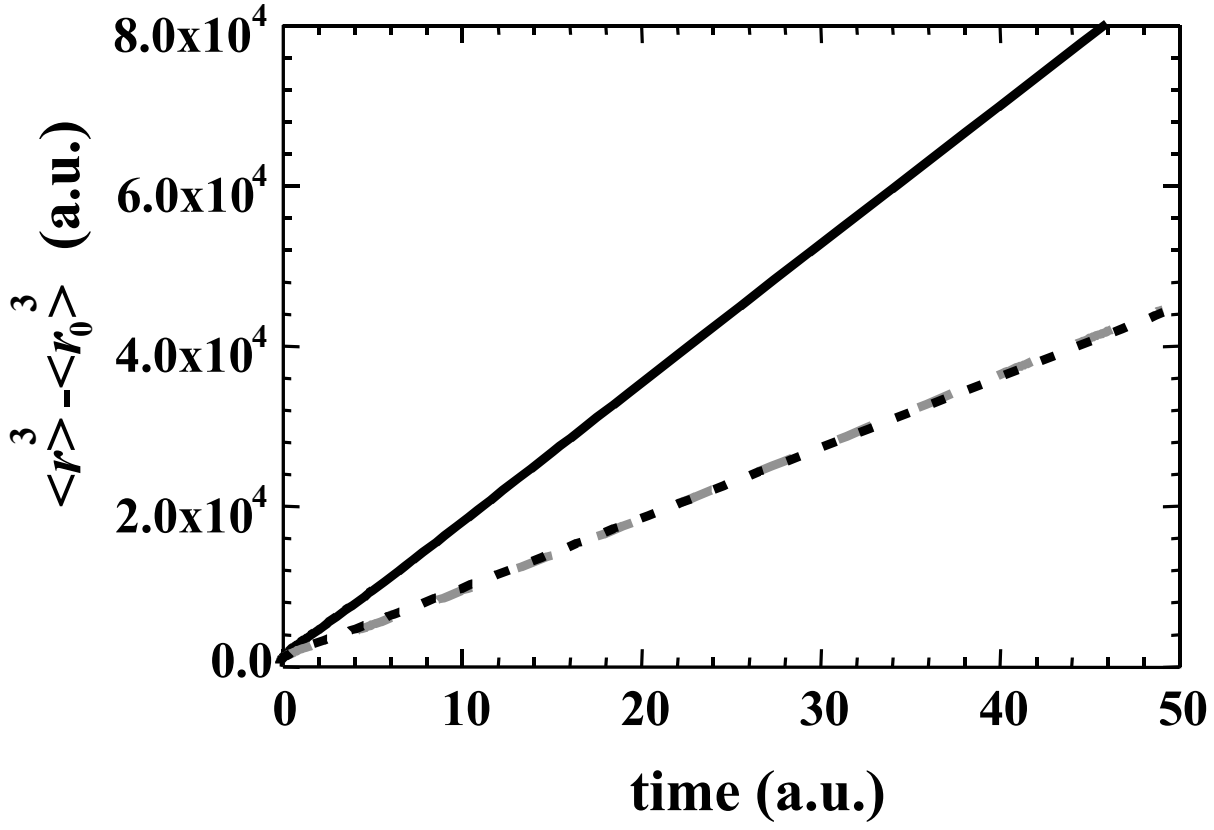
8.0x10^4
6.0x10^4
4.0x10^4
2.0x10^4
0.0
<r^3> - <r_0^3> (a.u.)
0
10
20
30
40
50
time (a.u.)

Figure 4.

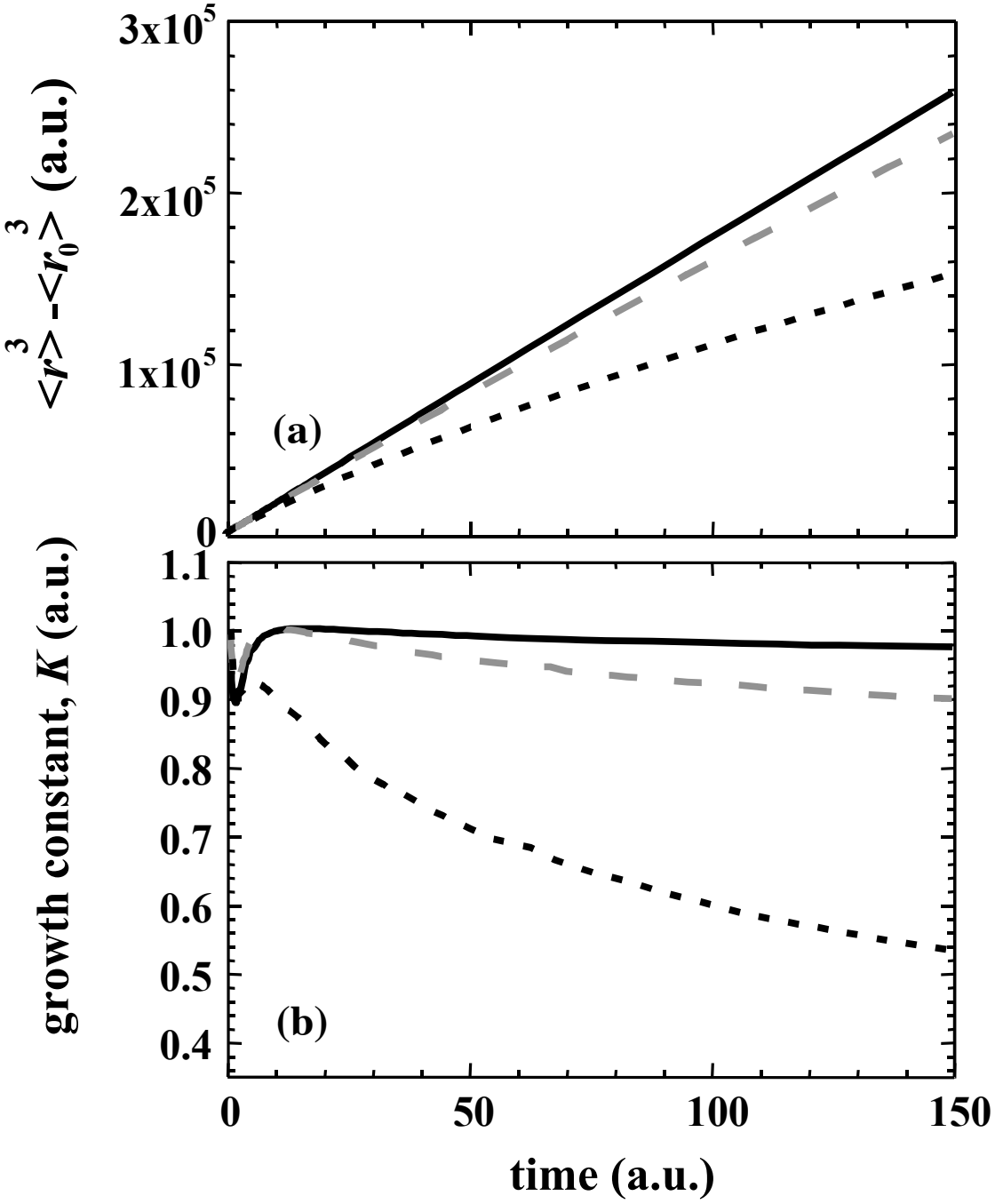
3x10^5
2x10^5
1x10^5
0
<r^3> - <r_0^3> (a.u.)
(a)
1.1
1.0
0.9
0.8
0.7
0.6
0.5
0.4
growth constant, K (a.u.)
(b)
0
50
100
150
time (a.u.)

Figure 5.